NJC

ROYAL SOCIETY OF CHEMISTRY

PAPER

View Article Online
View Journal | View Issue

Cite this: *New J. Chem.*, 2025, 49, 6535

Designing lenalidomide cocrystals with an extended-release profile for improved pulmonary drug delivery†

Martin A. Screen, [a] Gary Tomkinson,[b] James F. McCabe,[b] Sean Askin,[c] Clare S. Mahon, [a] Mark R. Wilson [a] and Jonathan W. Steed *[a]

Received 31st January 2025,
Accepted 31st March 2025

DOI: 10.1039/d5nj00425j

rsc.li/njc

Lenalidomide is a poorly soluble immunomodulatory drug that has been the subject of several cocrystal studies aiming to improve oral bioavailability by enhancing solubility. In contrast, for application in pulmonary fibrosis, reduced solubility may extend the retention time and reduce potential side effects of inhalable formulations. In this article, we present a proof-of-principle study on a low-solubility cocrystal of lenalidomide and melamine. The structure of the hydrated cocrystal was determined by single crystal X-ray diffraction and revealed a 3-dimensional hydrogen-bonding network between lenalidomide, melamine and channel-included solvent. The cocrystal has a lower maximum solubility than pure lenalidomide, making it more suitable for inhalable formulation approaches. A preliminary study shows that the cocrystal can be micronized with lactose as a model excipient with particle sizes in the appropriate order of magnitude for use in an inhalable formulation.

Introduction

Pharmaceutical cocrystals are used to improve the chemical, physical and economic characteristics of an active pharmaceutical ingredient (API) without modifying its chemical structure or pharmacology, by crystallising it with at least one other component or "coformer".[1–3] Unlike pharmaceutical salts, which have been used for decades to improve physicochemical properties such as the water solubility, toxicity profile and dissolution rate of APIs,[2] cocrystals consist of neutral components interacting non-covalently *via* hydrogen-bonds, π–π stacking, van der Waals forces and halogen bonds without electrostatic attraction between oppositely charged ions. Use of these interactions potentially allows new pharmaceutical solids with desirable physicochemical properties to be designed *via* a crystal engineering approach, using an understanding of possible supramolecular motifs between two or more components.[1,4] This "supramolecular synthon" approach to cocrystal design has proven effective for improving the pre-clinical properties of numerous poorly soluble drugs such as the anti-epileptic agent lamotrigine,[5] the anti-bacterial drug norfloxacin[6] and the anti-inflammatory drug indomethacin.[7] Solubility enhancement is not the only application for cocrystal formation, however. Work by Aakeröy, for example, has shown that solubility reduction by cocrystal formation can be highly effective in slow-release formulations such as agrochemicals.[8]

Lenalidomide (Scheme 1a), an immunomodulatory drug analogous to thalidomide, is primarily used for the treatment of multiple myeloma in an oral formulation where bioavailability can be improved by enhancing solubility.[9] Lenalidomide can also be used to treat pulmonary fibrosis,[10] where a lower solubility is often advantageous for producing lower and flatter drug dissolution profiles in the lungs.[11] As well as the

[a] *Durham University, Department of Chemistry, South Road, Durham, DH1 3LE, UK. E-mail: jon.steed@durham.ac.uk*
[b] *Early Pharmaceutical Development & Manufacture, Pharmaceutical Sciences, R&D, AstraZeneca, Macclesfield, SK10 2NA, UK*
[c] *Advanced Drug Delivery, Pharmaceutical Sciences, R&D, AstraZeneca, Cambridge, CB2 0AA, UK*

† Electronic supplementary information (ESI) available: Full crystallographic data, parameters of refinement and the hydrogen-bonding distances and angles; additional XRPD patterns and ^{1}H NMR spectra; additional DSC thermograms; additional VT-XRPD patterns and DVS isotherms. CCDC 2402673. For ESI and crystallographic data in CIF or other electronic format see DOI: https://doi.org/10.1039/d5nj00425j

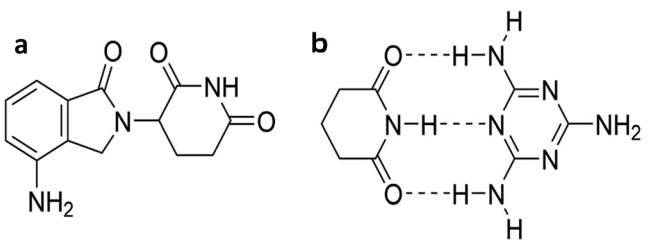

Scheme 1 Chemical structures of (a) lenalidomide and (b) a $2R_2^2(8)$ triple hydrogen-bonding synthon[20] with melamine.

commercially available hemihydrate Form B, lenalidomide can crystallize as the anhydrous Form A, the dihydrate Form E and several metastable anhydrous polymorphs accessible by different methods of dehydrating Form B or Form E.[12,13] The commercial form, marketed as Revlimid®, is designated as BCS Class 3 by the FDA with poor oral bioavailability resulting from a low permeability,[14] and the API has an approximate aqueous solubility of 0.5 mg mL^{-1} at neutral pH. The imide moiety within its structure makes lenalidomide a promising candidate for the design of cocrystals with amide-, carboxylic acid- and hydroxyl-containing coformers *via* hydrogen-bonding synthons involving N–H···O=C and C=O···H–O interactions. At least one of these synthons is present in each of the single crystal X-ray diffraction (XRD) structures of the five lenalidomide cocrystals in the Cambridge Structural Database (CSD).[15,16] A total of eighteen cocrystal forms (including their hydrates), three solvates and five salts of lenalidomide have been reported after extensive screening with generally recognized as safe (GRAS) compounds.[15–19] Cocrystals with 3,5-dihydroxybenzoic acid were shown to have approximately 40% higher maximum solubility in 0.2 M phosphate buffer at pH 6.8 and 37 °C compared to Form B, reaching the maximum solubility within 3 minutes before slowly decreasing over 24 hours as per the "spring and parachute effect" which many pharmaceutical cocrystals exhibit.[16] A cocrystal with nicotinamide was also synthesized following its prediction using a model of hydrogen-bond propensity (HBP) to screen for potential lenalidomide cocrystals. Not only does the cocrystal show a dissolution and solubility improvement over the pure API, but similar results were obtained for a physical mixture of the API and coformer, indicating the formation of a 1:1 complex in the dissolution media.[17] The coformers used in these examples all have aqueous solubilities one to three orders of magnitude greater than lenalidomide.

Compared to other non-parenteral administration methods, pulmonary drug delivery systems benefit from targeted delivery, reduced side effects and improved bioavailability due to the rate of absorption into the systemic circulation.[21] Inhaled drugs first dissolve in the aqueous lung lining fluid before they can translocate into the blood, lymph and cells, but if the diffusion is too rapid then the duration of pulmonary exposure and total pharmacological effect is diminished.[11] Extending the retention time of drug particles in the lungs is therefore favourable to reduce the frequency of doses that a patient is required to take. Poorly water-soluble drugs such as fluticasone propionate and several sex steroids and antifungal drugs exhibit slow absorption rates from the lungs because they dissolve slowly in the aqueous lung lining fluid, leading to prolonged drug exposure.[11,21,22] For particularly insoluble drugs, however, formulation as multicomponent solids with a highly soluble coformer has been demonstrated as an effective strategy for increasing drug dissolution rates and enhancing pulmonary drug release. Micronised cocrystals of the highly insoluble (<1 μg mL^{-1}) antifungal drug itraconazole with succinic acid and L-tartaric acid displayed up to 10-times higher intrinsic dissolution rates and pulmonary absorption profiles in rats compared to the amorphous spray-dried formulation and crystalline form of the pure drug with comparable particle sizes,[23] and the first cocrystal developed of RNA antiviral drug remdesivir with salicylic acid displayed an approximate 15-fold increase in drug release compared to the pure drug after 2 hours of dissolution in simulated lung fluid.[24] In contrast, a typical lenalidomide dose of 10 mg per day for pulmonary therapy[25] may dissolve quickly in the 10–30 mL volume of lung fluid usually present in humans,[26] therefore reducing the solubility and absorption rate of the drug in the lungs by formulating as a multicomponent solid with a low-solubility coformer may reduce the reported symptoms of coughs and fever arising from lenalidomide toxicity,[25] potentially improving its effectiveness as a treatment for pulmonary fibrosis.[27]

The imide group in lenalidomide consists of two carbonyl hydrogen-bond acceptors (A) separated by an N–H hydrogen-bond donor (D) in an A–D–A configuration, making it complementary to a molecule with a D–A–D configuration. An intuitive choice for a low-solubility coformer with a D–A–D configuration is melamine, a compound that is safe to use at low concentrations (<0.2 mg kg^{-1}) in humans,[28,29] with a reported aqueous solubility of 3.2 mg mL^{-1}.[30] This relatively low solubility coupled with the anticipated strong ADA–DAD hydrogen bonding pairing might be anticipated to give rise to a reduced solubility lenalidomide cocrystal. The triple hydrogen-bonding synthon between melamine and imide-containing cyanuric acid has already been exemplified in work by Seto and Whitesides[31] and by Wang *et al.* in the crystal structure of the melamine cyanuric acid complex (1:1) trihydrochloride.[32] It has also been used in the sonochemical preparation of hydrogels with uric acid.[33] Unlike all previously reported coformers of lenalidomide which contain alcohol, carboxylic acid, pyridyl and/or amide moieties as hydrogen-bond donors and acceptors, melamine contains three primary amine hydrogen bond donors as well as three triazine nitrogen atom acceptors. In the present work we report the design, preparation and properties of a reduced solubility cocrystal between lenalidomide and melamine that serves as a model exemplar of the way in which cocrystal engineering could be used to lower drug solubility for improved pulmonary therapy.

Experimental section

Materials and general methods

Lenalidomide (as the hemihydrate Form B[12]) and all coformers were purchased from Merck. Form A was obtained by drying Form B in an oven at 150 °C for 6 hours and characterized by XRPD. Infrared spectra were recorded between 4000 and 550 cm^{-1} using a PerkinElmer 100 FT-IR spectrometer with a uATR attachment. Unless otherwise specified, powder X-ray diffraction (XRPD) patterns were collected at room temperature using a Bruker AXS D8 Advance GX003410 diffractometer with a Lynxeye Soller PSD detector, using Cu Kα radiation at a wavelength of 1.5406 Å and collecting from $2^\circ \leq 2\theta \leq 40^\circ$.

Preparation of lenalidomide melamine non-stoichiometric hydrate (1)

Lenalidomide Form B (278 mg, 1.00 mmol) and melamine (240 mg, 1.90 mmol) were added in excess to water (40 mL)

such that the undissolved solid contained a 1 : 1 molar ratio of the two components and stirring overnight. The resulting solid was filtered and dried to afford cocrystal **1** as a white powder (300 mg, 0.728 mmol, 73%). Cocrystal **1** can also be prepared by manual grinding of lenalidomide Form B and melamine in a pestle and mortar (Fig. S1, ESI†).

Preparation of lenalidomide melamine methanol hemihydrate (2)

Lenalidomide Form B (230 mg, 0.857 mmol) and melamine (108 mg, 0.857 mmol) were added to methanol (350 mL), stirred to dissolve, and the solvent was slowly evaporated to afford lenalidomide melamine methanol hemihydrate (cocrystal **2**) as blue-green needles (225 mg, 0.528 mmol, 62%). Cocrystal **2** can also be prepared using a liquid-assisted grinding (LAG) method, by mixing lenalidomide Form B and melamine in a 1 : 1 molar ratio with 2 drops of methanol in a 5 mL stainless steel grinding jar with one stainless steel grinding ball (6.4 mm diameter) and grinding with a Retsch MM200 Mixer Mill at a frequency of 20 Hz for 30 minutes. The resulting solid was analyzed by IR spectroscopy and XRPD (Fig. S2, ESI†).

Single crystal X-ray diffraction (SC-XRD)

Single-crystal X-ray diffraction data for cocrystal **2** was collected at 120 K using Mo Kα radiation at a wavelength of 0.71073 Å on a Bruker D8 Venture 3-circle diffractometer. The structure was solved by direct methods and refined by full-matrix least squares on F^2 for all data using Olex2[34] and SHELXTL.[35] All non-hydrogen atoms were refined in anisotropic approximation, while hydrogen atoms were placed in the calculated positions and refined in riding mode. Crystal data for **2**: $C_{17}H_{24}N_9O_{4.5}$, M_r = 426.45, space group $P\bar{1}$, a = 7.9402(3) Å, b = 10.2062(3) Å, c = 12.5527(4) Å, α = 93.5640(10) °, β = 94.6780(10) °, γ = 111.0870(10) °, V = 941.39(5) Å^3, R_1 ($I > 2s(I)$) = 0.0800, wR_2 (all data) = 0.1816. Full crystallographic data, parameters of refinement and the hydrogen-bonding distances and angles are listed in Tables S1 and S2 (ESI†). The structure was deposited in the CCDC under deposition number 2402673.

Thermal analysis

Differential scanning calorimetry (DSC) samples were prepared using Tzero standard pans and lids and analyzed using a TA instruments Q2000 differential scanning calorimeter by first equilibrating at 25 °C and then heating to 400 °C at 10 °C min^{-1}. Heat–cool–heat DSC samples were heated first to 220 °C, cooled back down to 25 °C, then heated again to 400 °C. Modulated DSC samples were first equilibrated at 25 °C then heated to 350 °C using a modulated method with a scanning speed of 3 °C min^{-1}, an amplitude of ±1 °C and a period of 60 s. The instrument was calibrated using an indium standard prior to analysis, with a melting point onset of 156.89 °C and a heat capacity of 33.971 J g^{-1}. Thermogravimetric analysis (TGA) samples were analyzed using platinum pans and a TA instruments discovery thermogravimetric analyzer, heating from 25 °C to 400 °C at 10 °C min^{-1}.

Variable temperature X-ray diffraction (VT-XRD)

VT-XRD powder patterns using a Bruker D8 Advance A25 diffractometer with a Lynxeye detector and an Anton Paar HTK 1200N furnace, using Cu Kα radiation at a wavelength of 1.5406 Å and collecting from $4^\circ \leq 2\theta \leq 40^\circ$.

Dynamic vapor sorption (DVS)

Vapor sorption isotherms were measured by dynamic vapor sorption (DVS) at 25 °C using a dynamic vapor sorption resolution instrument (Surface Measurement System, UK). The relative humidity (RH) was then increased in increments of 10% RH, starting from 40% RH up to 90% RH, returning to 0% RH, increasing again to 90% RH, and finally returning to 0% RH. The waiting time for 0.001% weight change was set to 30 min and the further step was increased or decreased automatically.

Ultra performance liquid chromatography (UPLC) analysis

The concentrations of lenalidomide were determined using a Waters ARC UPLC-MC206 system with an ACQUITY UPLC BEH C18 column (130 Å, 1.7 μm, 2.1 mm × 50 mm, Waters Corporation, UK) and a UV detection wavelength of 305 nm. The mobile phase of acetonitrile/water was varied in a gradient method from 95/5 v/v to 5/95 v/v at a flow rate of 1 mL min^{-1}.

Lenalidomide solubility

The thermodynamic solubility of lenalidomide Form A in phosphate buffered saline (PBS) was determined by adding an excess of Form A solid to 1 mL of solvent and stirring at 1000 rpm for 24 hours. The samples were then centrifuged for 30 minutes at 31 000 × g and the supernatant was diluted appropriately to maintain absorbance readings within the UPLC standard curve. The concentration of lenalidomide was determined by UPLC analysis, converting peak area values to concentrations *via* a calibration curve.

Non-sink dissolution measurements

Cocrystal **1** and lenalidomide Form A were ground to powders and consistent particle sizes were confirmed by optical microscopy. A physical mixture of Form A and melamine was prepared by stirring the two powders together in a 1 : 1 molar ratio without grinding and characterized by XRPD prior to dissolution. Dissolution experiments were run in triplicate for each sample. Vessels were charged with approximately 5 mL of pre-warmed PBS at 37 °C before accurately weighed masses of each sample were added such that all slurries were at ten times the measured solubility limit of lenalidomide. Slurries were stirred at 350 rpm for 24 hours. Aliquots of the slurries were removed at each time point, centrifuged for 30 minutes at 31 000 × g, and the supernatant was diluted appropriately to maintain absorbance readings within the UPLC standard curve. The concentrations were determined by UPLC analysis, converting peak area values to concentrations *via* a calibration curve. The solids obtained by centrifugation of the 2-hour and 24-hour aliquots were dried and analyzed by XRPD.

Scanning electron microscopy (SEM)

SEM samples were prepared by adding solid powders to polycarbonate wafers and coating with 25 nm of platinum using a Cressington 328 Ultra High-Resolution EM Coating System.

The images were obtained using a Carl Zeiss Sigma 300 VP FEG SEM microscope, operated at 5 kV using an in-lens detector.

Micronization and conditioning

Cocrystal **1** was milled both alone and at 20% w/w with α-lactose in a 5 mL stainless steel grinding jar with one stainless steel grinding ball (6.4 mm diameter) using a Retsch MM200 Mixer Mill at a frequency of 20 Hz for 30 minutes. The resulting solids were analyzed by XRPD, modulated DSC and SEM. The samples were then conditioned in a desiccator at 50 °C and 75% RH using a saturated NaCl solution,[36] and the resulting solids were analyzed again by XRPD, modulated DSC and SEM.

Results and discussion

A hydrated lenalidomide melamine cocrystal (**1**) can be prepared by mechanochemical methods such as grinding lenalidomide Form B and melamine by hand in a pestle and mortar or in a ball mill without addition of solvent, or by slurrying lenalidomide Forms A or B and melamine in water. Mechanochemical grinding of the anhydrous lenalidomide Form A with melamine, however, fails to produce a cocrystal and results in a physical mixture of the two components. This indicates the importance of hydration in the formation of stable cocrystal **1**. While single crystals of **1** could not be obtained, single crystals can be grown of a closely related lenalidomide melamine cocrystal as a mixed methanol and water solvate (**2**) by slow evaporation from methanol. The same mixed solvate form can also be obtained as a powder by liquid-assisted grinding of lenalidomide Form B and melamine in the presence of methanol. The XRPD patterns of cocrystals **1** and **2** are identical indicating that the two forms are isostructural, and XRPD and ^{1}H NMR analysis (Fig. S3 and S4 respectively, ESI†) shows that a slurry of cocrystal **2** in water leads to the removal of methanol from the cocrystal to give **1** without affecting the crystal structure. Leaving cocrystal **2** in open air for several days also allows all the methanol to evaporate from the crystals without affecting the X-ray powder pattern. Cocrystals **1** and **2** contain a 1 : 1 ratio of lenalidomide and melamine even though a 3 : 1 cocrystal might be expected based on the three-fold symmetry of melamine with a D–A–D hydrogen bonding motif available on each face. Grinding both components together in either a 1 : 1 or 3 : 1 molar ratio gives the same solvated 1 : 1 cocrystal structure. This may be because the putative 3 : 1 hydrogen-bonded unit of lenalidomide and melamine packs poorly in the crystalline phase compared to the 1 : 1 cocrystal where interactions with solvent satisfy the hydrogen-bonding capacity of the remaining melamine donors and acceptors (Fig. 1).

Single crystal X-ray structure determination of cocrystal **2** shows it to be a mixed solvate of the 1 : 1 lenalidomide melamine cocrystal, containing one mole of methanol and 0.5 moles of water. Lenalidomide and melamine molecules are linked by a triple hydrogen-bonding synthon N2–H2···N4, N8–H8C···O2 and N7–H7A···O3, and form a chain along the crystallographic *a* axis. Neighboring antiparallel chains along *a*

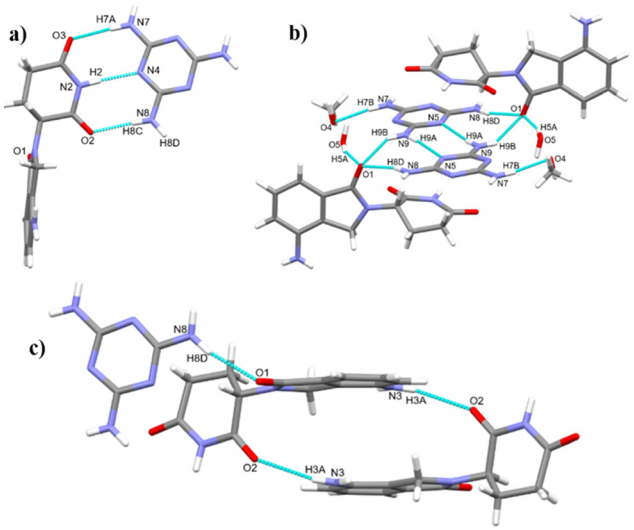

Fig. 1 The hydrogen-bonding motifs that comprise the 3-dimensional structure of **2**. (a) A $2R_2^2(8)$ triple hydrogen-bonding synthon links lenalidomide and melamine in chains along the *a* axis with an N7···O3 distance of 3.007(3) Å and an N8···O2 distance of 2.924(3) Å. (b) Neighboring antiparallel chains are connected along the *b* axis by interactions between melamine molecules and with solvent in channels aligned with the *a* axis. The majority component of the disordered methanol solvent is shown. (c) Lenalidomide molecules interact with each other and with melamine *via* hydrogen-bonds along the *c* axis, as well as forming π···π interactions between lenalidomide molecules aligned with the *b* axis.

are connected along the *b* axis by $R_2^2(8)$ synthons between melamine molecules from opposing chains (N9–H9A···N5), N9–H9B···O1 interactions linking melamine and lenalidomide molecules from opposing chains, and N3–H3A···O5 interactions between lenalidomide and water altogether producing a 2D sheet. The 2D structure is further supported through π···π interactions between lenalidomide molecules in neighboring antiparallel chains, with a centroid–centroid distance of 3.60 Å. Along the *c* axis, melamine interacts with lenalidomide *via* N8–H8D···O1 and with methanol *via* N7–H7B···O4 interactions and lenalidomide molecules are linked *via* N3–H3A···O2, generating a 3D structure. The methanol and water molecules occupy channels that run along the *a* axis, and the methanol molecules are disordered. XRPD analysis of the bulk sample is consistent with the calculated XRPD pattern from the single crystal data, confirming bulk solid form purity (Fig. 2). This powder pattern also matches with cocrystal **1**, containing no methanol.

While methanol is included in the channel solvate structure upon recrystallizing **2** by slow evaporation from methanol, it is not present in the isostructural crystal **1** produced by grinding or slurry of lenalidomide Form B and melamine in water, indicating that it is not necessary for the stability of the cocrystal and can be replaced with water without disrupting the rest of the structure. This is crucial for the pharmaceutical developability of the cocrystal, since methanol solvates are classified as having inherent toxicity.[37] The remainder of this work is concerned only with cocrystal **1**, although full thermal characterization of cocrystal **2** is included in ESI† (Fig. S5–S8). Furthermore, a hypothetical pulmonary therapy dose of cocrystal **1** containing 10 mg of

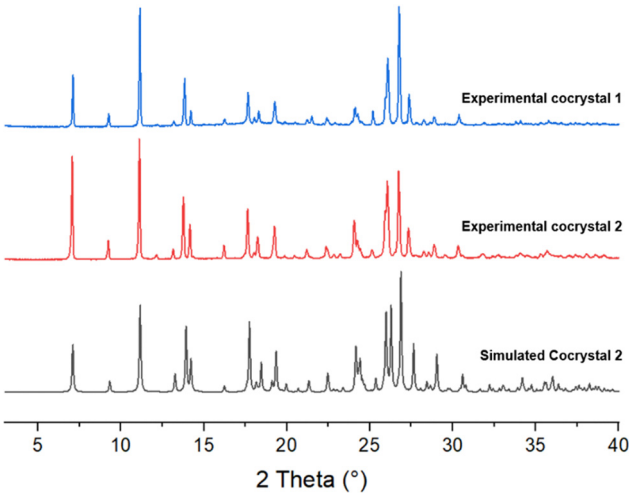

Fig. 2 XRPD pattern simulated from the SC-XRD structure of **2** compared to the bulk experimental samples of cocrystals **1** and **2**.

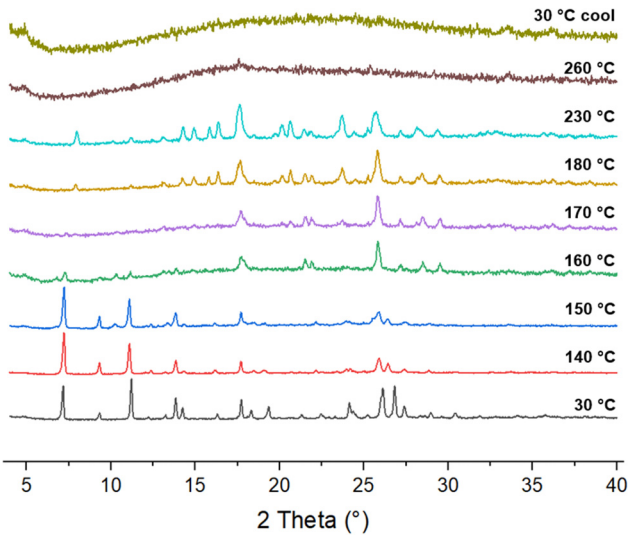

Fig. 4 VT-XRD patterns for **1** showing recrystallization into lenalidomide Form A above 150 °C, which melts to leave amorphous material at 260 °C.

lenalidomide active ingredient[25] would only contain approximately 5 mg of melamine, which is safe for once-daily consumption in humans weighing at least 25 kg based its tolerable daily intake.[28,29]

A broad and shallow endotherm up to 110 °C in the DSC thermogram (Fig. 3) corresponds to a 6.7% change in mass in the TGA trace, suggesting that the water in cocrystal **1** is relatively labile and is initially present in a molar ratio of approximately 1.5 : 1 with lenalidomide, indicating that **1** is a non-stoichiometric hydrate. The dehydrated cocrystal appears to melt at 159 °C before recrystallizing into lenalidomide Form A at 182 °C, followed by the melt of Form A at 250 °C, as supported by VT-XRD analysis (Fig. 4). While Form A typically melts at 270 °C,[12] the presence of melamine as an impurity in the lenalidomide sample as well as the likelihood of poor-quality crystals forming *in situ* are potential causes of the observed melting point depression. Melamine appears to be amorphous after the recrystallisation of lenalidomide given the absence of its characteristic peaks in the VT-XRD patterns above 180 °C, however no glass transition is observed between 25 and 220 °C in the heat–cool–heat DSC experiment (Fig. S9, ESI†). A glass transition for amorphous melamine was observed, however, at 137 °C for the analogous heat–cool–heat DSC experiment on cocrystal **2** (Fig. S7, ESI†). DVS analysis (Fig. S10, ESI†) shows that **1** loses 6.8% mass when decreasing from 40 to 0% RH, closely matching the solvent loss observed by TGA and indicating that below 10% RH, **1** becomes a fully dehydrated solvate. An increase of 3.9% mass when ramping up from 40 to 90% RH indicates that additional water can pack into the solvent channels at high humidity, leading to a structure of **1** with a 2.5 : 1 molar ratio of water in the asymmetric unit. The absence of hysteresis in the DVS isotherm indicates that the cocrystal structure remains intact throughout the sorption and

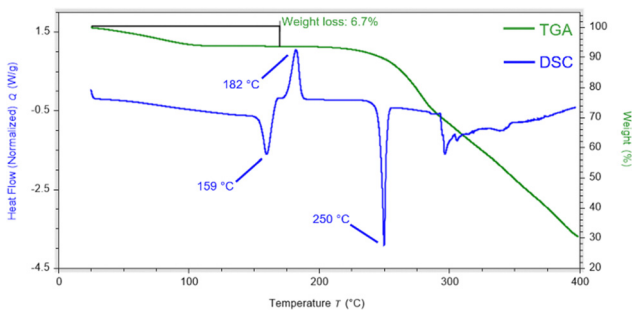

Fig. 3 DSC and TGA thermograms for **1** showing a broad solvent loss endotherm up to approximately 110 °C followed by the melt of the resulting dehydrated cocrystal at 159 °C, its subsequent recrystallisation into lenalidomide Form A at 182 °C and the melt of Form A with an onset temperature of 246 °C and a peak at 250 °C. Melamine appears to decompose at approximately 300 °C.

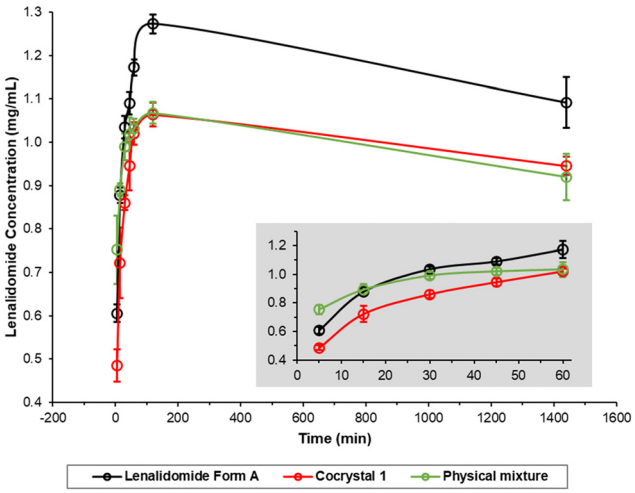

Fig. 5 Non-sink powder dissolution profiles of lenalidomide Form A, **1** and a physical mixture of Form A and melamine (PM) over 24 hours in PBS at 37 °C. Dissolution experiments were run in triplicate with error bars displaying the standard error values. The inlaid plot shows the first hour of the dissolution profile.

desorption cycles and is consistent with the channel solvate structure observed in the X-ray structure determination of **2**.

Fig. 5 shows non-sink dissolution profiles for **1** in phosphate buffered saline (PBS) compared to lenalidomide Form A, which quickly converts to Form B in aqueous solution and has a similar dissolution profile,[38] and a physical mixture of Form A with melamine (PM). PBS is a common dissolution medium employed in research studies focusing on pulmonary drug delivery.[39,40] All three samples reach their maximum solubility value between 1–2 hours. The maximum solubility value for **1** is approximately 20% lower than Form A, which may indicate that it has a greater lattice energy and therefore a greater thermodynamic barrier to dissolution, and/or because it is a hydrate, which typically have lower water solubility than anhydrous forms.[12,38] The significant decrease in the Form A solubility between 2 and 24 hours can also be attributed to the partial conversion of Form A into the dihydrate Form E in aqueous suspension, confirmed by XRPD analysis of solids removed at the 2- and 24-hour timepoints (Fig. 6). The PM samples begin with a similar dissolution profile to the pure Form A sample but the solubility plateaus within the first hour and then follows the same dissolution profile as **1**. XRPD analysis (Fig. 6c) shows that the PM samples contain mostly **1** with traces of Form B after 2 hours and remain the same until the 24-hour timepoint. This demonstrates the strength of the interactions in the cocrystal and how quickly this cocrystal form can be obtained by slurrying in aqueous solution. XRPD analysis shows that cocrystal **1** is stable over the 24-hour period, including the PM samples where **1** is produced *in situ*. The lower solubility and greater physical stability against recrystallisation of **1** may be advantageous for inhaled formulations of lenalidomide for the treatment of pulmonary fibrosis since these properties extend the duration of pulmonary exposure and increase the overall pharmacological effect,[11] while reducing unwanted side effects such as irritancy. While not relevant to pulmonary drug delivery, the same dissolution behavior is observed over 24 hours of the same dissolution experiment in fasted state simulated intestinal fluid (FaSSIF) where the maximum solubility of **1** is approximately 60% lower than lenalidomide Form A, indicating that these results are general across more than one bio-relevant medium (Fig. S11, ESI†).

Dry powder inhalable drug formulations require particle sizes between 1–5 μm to reach the alveolar region of the lungs and have their optimum therapeutic effect. To assess the feasibility of using cocrystal **1** as an inhalable drug, the cocrystal was micronized on its own and separately in the presence of α-lactose (lactose monohydrate), the most common excipient in pulmonary drug delivery.[41] A 20% w/w loading of cocrystal **1** was used such that the resulting micronized mixture with lactose would contain 12.5% w/w of the lenalidomide API. The micronized powders were characterized by XRPD before and after 24 hours of conditioning in a desiccator at 50 °C and 75% RH to emulate a typical industrial procedure. The powder diffractograms (Fig. 7) show that cocrystal **1** is considerably amorphized after milling, but its crystallinity is at least partially restored after conditioning. This is confirmed by modulated DSC (Fig. S12, ESI†) which shows a glass transition (T_g) at

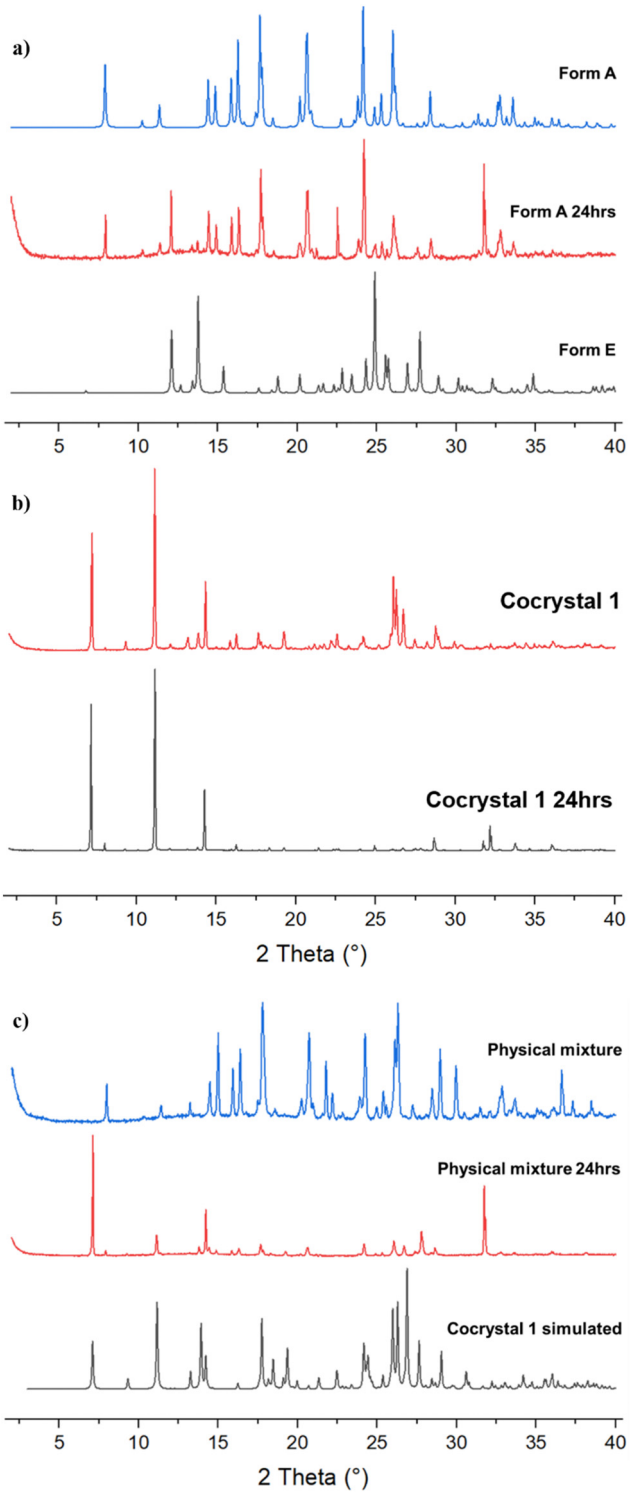

Fig. 6 XRPD patterns comparing the powder samples before and after 24 hours of dissolution in PBS at 37 °C. (a) Form A converts partially into Form E over 24 hours. (b) **1** remains the same form over 24 hours. (c) A physical mixture of Form A and melamine converts into **1** over 24 hours.

143 °C followed by a recrystallization event and the melt of lenalidomide, as before in Fig. 3. The sample containing α-lactose shows hardly any peaks corresponding to cocrystal **1** between milling and conditioning since it is only present at

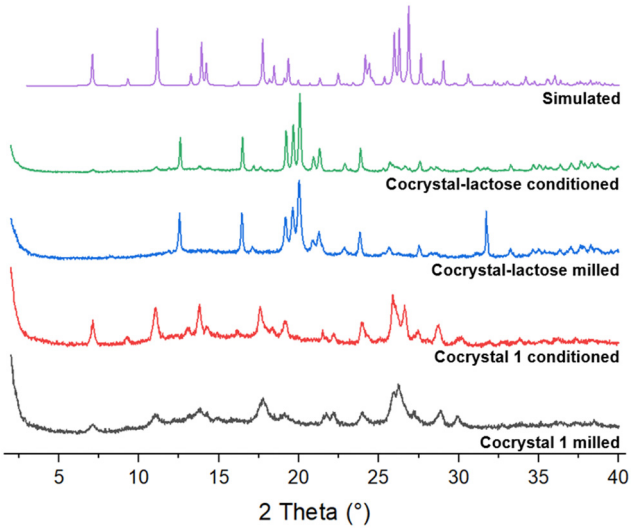

Fig. 7 XRPD patterns comparing cocrystal **1** after micronization by milling with and without α-lactose as a model excipient, and after a subsequent 24-hour conditioning step at 50 °C and 75% RH. The stronger peaks observed in the cocrystal-lactose samples correspond to α-lactose. The crystallinity of cocrystal **1** appears to decrease significantly after milling but is partially restored after conditioning. The simulated diffractogram is that of cocrystal **1** from the single crystal structure.

20% w/w and considerably amorphized, but some small peaks are more prominent after conditioning. The modulated DSC thermograms of the lactose-containing samples (Fig. S13, ESI†) are dominated by the dehydration and degradation endotherms of α-lactose, obscuring any thermal events corresponding to cocrystal **1**.

The micronized cocrystal **1**, which still contains the water present from the hydrate crystals that were milled, does not appear to recrystallize over 7 days in the same way if left open to air, indicating that the elevated temperature in the conditioning step is likely to be the critical factor in the recrystallisation of cocrystal **1**.

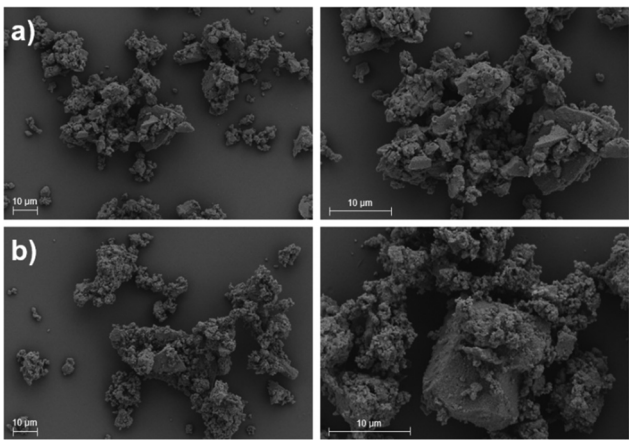

Fig. 8 SEM images of cocrystal **1** after milling for 30 minutes and conditioning at 50 °C and 75% RH for 24 h (a) API alone and (b) with α-lactose at 20% w/w of the cocrystal.

SEM images (Fig. 8) show that the particles of cocrystal **1** micronized alone are mostly 5–20 μm in diameter, although some particles appear to be clumps of agglomerated particles as small as 1 μm and some single particles are as large as 50 μm, which are an order of magnitude too large for pulmonary delivery. It is unclear whether the particles have agglomerated before or during the platinum coating process to prepare the SEM samples. Particles of cocrystal **1** micronized with α-lactose are similarly sized although the surfaces of larger particles appear to be coated with much finer particles, some of which are under 1 μm. Agglomeration is also observed in the lactose-containing samples. This demonstrates that producing particles of cocrystal **1** and a model excipient within the appropriate size range for use in an inhalable formulation is feasible by simply milling, although the milling process would have to be optimized to reduce the size of the largest particles which would be at risk of impacting the mouth and the walls of the higher airways.[42] Furthermore, it is not obvious whether the residual amorphous material observed by XRPD and DSC is heterogeneously dispersed as separate amorphous particles amongst the crystalline particles, or whether it uniformly coats the exterior of each crystalline particle. In the latter case, the stickier and more hygroscopic amorphous surfaces can increase bridging between particles and lead to the formation of larger and less inhalable agglomerates.[43] Recrystallization of the amorphous solid coating the particles may also cause them to grow beyond the desirable size range.

Non-sink dissolution profiles of cocrystal **1** before and after the micronization and conditioning step were measured in PBS at 37 °C using the same procedure as to compare cocrystal **1** with lenalidomide Form A (Fig. S14, ESI†). The profiles for both samples are indistinguishable, suggesting that like the physical mixture of Form A and melamine in Fig. 5, the amorphous solid rapidly recrystallises into cocrystal **1** within the aqueous slurry.

Conclusions

A cocrystal of lenalidomide and melamine was designed by the supramolecular synthon approach and synthesized. The cocrystal is based on the triple hydrogen-bond ADA-DAD synthon anticipated between lenalidomide and melamine but forms a 1:1 cocrystal rather than 3:1, with additional channel-included solvent. Thermal and dynamic vapor sorption analysis show that the channel solvent is labile and a dehydrated cocrystal is stable at low humidity and room temperature, but is unstable at elevated temperature in the DSC, converting to lenalidomide Form A. Cocrystal **1** has a lower maximum solubility than Form A by approximately 20% in PBS and 60% in FaSSIF and is stable against recrystallisation into lenalidomide or its hydrates over a 24-hour dissolution experiment. A preliminary study shows that simply grinding **1** with α-lactose in a ball mill can produce particles of a size within the appropriate order of magnitude for use in an inhalation device, without irreversibly destroying the crystal structure or affecting the dissolution properties. Designing cocrystals of drugs with

lower solubility coformers *via* the supramolecular synthon approach may be a useful strategy for improving inhalable formulations of lenalidomide for treating pulmonary fibrosis.

Data availability

Full crystallographic data, parameters of refinement and the hydrogen-bonding distances and angles; additional XRPD patterns and ^{1}H NMR spectra, additional DSC thermograms; additional VT-XRPD patterns and DVS isotherms are provided in ESI† (PDF). Underlying data for this work comprising XRPD, DSC, TGA, IR, UPLC and SEM can be obtained from: **https://doi.org/10.15128/r2zp38wc706**.

Conflicts of interest

There are no conflicts to declare.

Acknowledgements

M. A. S. thanks the Engineering and Physical Sciences Research Council and AstraZeneca for studentship funding *via* the Soft Matter and Functional Interfaces Centre for Doctoral Training (EP/S023631/1). We would also like to express thanks to Dr Dmitry Yufit and Dr Aileen Congreve (Department of Chemistry, Durham University) for invaluable assistance with crystallography and chromatography respectively.

References

1 D. J. Berry and J. W. Steed, Pharmaceutical cocrystals, salts and multicomponent systems; intermolecular interactions and property based design, *Adv. Drug Delivery Rev.*, 2017, **117**, 3–24.
2 S. M. Berge, L. D. Bighley and D. C. Monkhouse, Pharmaceutical Salts, *J. Pharm. Sci.*, 1977, **66**, 1–19.
3 P. L. Gould, Salt selection for basic drugs, *Int. J. Pharm.*, 1986, **33**, 201–217.
4 G. R. Desiraju, P. David, Y. Curtin, P. Lain and C. Paul, Supramolecular synthons in crystal engineering—a new organic synthesis, *Angew. Chem., Int. Ed. Engl.*, 1995, **34**, 2311–2327.
5 M. L. Cheney, N. Shan, E. R. Healey, M. Hanna, L. Wojtas, M. J. Zaworotko, V. Sava, S. Song and J. R. Sanchez-Ramos, Effects of crystal form on solubility and pharmacokinetics: A crystal engineering case study of lamotrigine, *Cryst. Growth Des.*, 2010, **10**, 394–405.
6 S. Basavoju, D. Boström and S. P. Velaga, Pharmaceutical cocrystal and salts of norfloxacin, *Cryst. Growth Des.*, 2006, **6**, 2699–2708.
7 S. Basavoju, D. Boström and S. P. Velaga, Indomethacin-saccharin cocrystal: Design, synthesis and preliminary pharmaceutical characterization, *Pharm. Res.*, 2008, **25**, 530–541.
8 B. Sandhu, A. S. Sinha, J. Desper and C. B. Aakeröy, Modulating the physical properties of solid forms of urea using co-crystallization technology, *Chem. Commun.*, 2018, **54**, 4657–4660.
9 D. V. Bhalani, B. Nutan, A. Kumar and A. K. Singh Chandel, Bioavailability enhancement techniques for poorly aqueous soluble drugs and therapeutics, *Biomedicines*, 2022, **10**, 9.
10 Z. Luo, L. Ji, H. Liu, Y. Sun, C. Zhao, X. Xu, X. Gu, X. Ai and C. Yang, Inhalation lenalidomide-loaded liposome for bleomycin-induced pulmonary fibrosis improvement, *AAPS PharmSciTech*, 2023, **24**, 1–14.
11 Y. Guo, H. Bera, C. Shi, L. Zhang, D. Cun and M. Yang, Pharmaceutical strategies to extend pulmonary exposure of inhaled medicines, *Acta Pharm. Sin. B*, 2021, **11**, 2565.
12 Polymorphic forms of 3-(4-amino-1-oxo-1,3 dihydro-isoindol-2-yl)-piperidine-2,6-dione, *US Pat.*, US 7,465,800 B2, 2008.
13 L. Jia, Z. Li and J. Gong, Two new polymorphs and one dihydrate of lenalidomide: solid-state characterization study, *Pharm. Dev. Technol.*, 2019, **24**, 1175–1180.
14 Lenalidomide immediate release formulations, *WIPO Pat.*, WO 2019/081749 A1, 2019.
15 J. X. Song, J. M. Chen and T. B. Lu, Lenalidomide-gallic acid cocrystals with constant high solubility, *Cryst. Growth Des.*, 2015, **15**, 4869–4875.
16 J. X. Song, Y. Yan, J. Yao, J. M. Chen and T. B. Lu, Improving the solubility of lenalidomide via cocrystals, *Cryst. Growth Des.*, 2014, **14**, 3069–3077.
17 L. Wang, Y. Yan, X. Zhang and X. Zhou, Novel pharmaceutical cocrystal of lenalidomide with nicotinamide: Structural design, evaluation, and thermal phase transition study, *Int. J. Pharm.*, 2022, **613**, 121394.
18 Crystalline forms of lenalidomide, *WIPO Pat.*, WO 2019/064222 A1, 2019.
19 Novel crystalline forms of 3-(4-amino-1-oxo-1,3 dihydro-isoindol-2-yl)-piperidine-2,6-dione, *US Pat.*, US 2014/0296291 A1, 2014.
20 M. C. Etter, Encoding and decoding hydrogen-bond patterns of organic compounds, *Acc. Chem. Res.*, 1990, **23**, 120–126.
21 J. S. Patton and P. R. Byron, Inhaling medicines: delivering drugs to the body through the lungs, *Nat. Rev. Drug Discovery*, 2007, **6**, 67–74.
22 J. Winkler, G. Hochhaus and H. Derendorf, How the lung handles drugs: pharmacokinetics and pharmacodynamics of inhaled corticosteroids, *Proc. Am. Thorac. Soc.*, 2004, **1**, 356–363.
23 M. Karashima, N. Sano, S. Yamamoto, Y. Arai, K. Yamamoto, N. Amano and Y. Ikeda, Enhanced pulmonary absorption of poorly soluble itraconazole by micronized cocrystal dry powder formulations, *Eur. J. Pharm. Biopharm.*, 2017, **115**, 65–72.
24 S. N. Wong, K.-H. Low, Y. L. Poon, X. Zhang, H. W. Chan and S. F. Chow, Synthesis of the first remdesivir cocrystal: design, characterization, and therapeutic potential for pulmonary delivery, *Int. J. Pharm.*, 2023, **640**, 122983.
25 K. Amraoui, K. Belhadj, B. Maître, C. Jannière-Nartey and J. Dupuis, Pulmonary toxicity after long-term treatment with

lenalidomide in two myeloma patients, *Eur. Respir. Rev.*, 2013, **22**, 93–95.
26 J. S. Patton, J. D. Brain, L. A. Davies, J. Fiegel, M. Gumbleton, K.-J. Kim, M. Sakagami, R. Vanbever and C. Ehrhardt, *J. Aerosol Med. Pulm. Drug Delivery*, 2010, **23**, 71–87.
27 J. A. Tolman and R. O. Williams, Advances in the pulmonary delivery of poorly water-soluble drugs: influence of solubilization on pharmacokinetic properties, *Drug Dev. Ind. Pharm.*, 2010, **36**, 1–30.
28 Melamine in Tableware Questions and Answers, **https://www.fda.gov/food/economically-motivated-adulteration-food-fraud/melamine-tableware-questions-and-answers**, (accessed August 2024).
29 EFSA cuts melamine TDI by 60 per cent, **https://www.feednavigator.com/Article/2010/04/15/EFSA-cuts-melamine-TDI-by-60-per-cent**, (accessed August 2024).
30 S. H. Yalkowsky, Y. He and P. Jain, *Handbook of Aqueous Solubility Data*, CRC Press, Boca Raton, 2nd edn, 2010.
31 C. T. Seto and G. M. Whitesides, Molecular self-assembly through hydrogen bonding: supramolecular aggregates based on the cyanuric acid melamine lattice, *J. Am. Chem. Soc.*, 1993, **115**, 905–916.
32 Y. Wang, B. Wei and Q. Wang, Crystal structure of melamine cyanuric acid complex (1:1) trihydrochloride, MCA·3HCl, *J. Crystallogr. Spectrosc. Res.*, 1990, **20**, 79–84.
33 K. M. Anderson, G. M. Day, M. J. Paterson, P. Byrne, N. Clarke and J. W. Steed, Structure calculation of an elastic hydrogel from sonication of rigid small molecule components, *Angew. Chem., Int. Ed.*, 2008, **47**, 1058–1062.
34 O. V. Dolomanov, L. J. Bourhis, R. J. Gildea, J. A. K. Howard and H. Puschmann, OLEX2: a complete structure solution, refinement and analysis program, *J. Appl. Crystallogr.*, 2009, **42**, 339–341.
35 G. M. Sheldrick, Crystal structure refinement with SHELXL, *Acta Crystallogr., Sect. C: Struct. Chem.*, 2015, **71**, 3–8.
36 A. Wexler and S. Hasegawa, Relative humidity-temperature relationships of some saturated salt solutions in the temperature range 0 to 50 C, *J. Res. Natl. Bur. Stand.*, 1954, **53**(1), 19–26.
37 Food and Drug Administration, Q3C-Tables and List Guidance for Industry 1, U.S. Department of Health and Human Services, United States, 2018.
38 Polymorphic forms of 3-(4-amino-1-oxo-1, 3 dihydroisoindo1-2-yl)-piperidine-2,6-dione, *US Pat.*, US 7,977,357 B2, 2011.
39 Y.-J. Son, M. Horng, M. Copley and J. T. McConville, Optimization of an In Vitro Dissolution Test Method for Inhalation Formulations, *Dissolution Technol.*, 2010, **17**(2), 6–13.
40 S. May, B. Jensen, C. Weiler, M. Wolkenhauer, M. Schneider and C.-M. Lehr, Dissolution Testing of Powders for Inhalation: Influence of Particle Deposition and Modeling of Dissolution Profiles, *Pharm. Res.*, 2014, **31**, 3211–3224.
41 G. A. Hebbink, M. Jaspers, H. J. W. Peters and B. H. J. Dickhoff, Recent developments in lactose blend formulations for carrier-based dry powder inhalation, *Adv. Drug Delivery Rev.*, 2022, **189**, 114527.
42 P. C. L. Kwok and H. K. Chan, Pulmonary drug delivery, *Ther. Delivery*, 2013, **4**, 877–878.
43 P. H. M. Janssen, L. M. N. Bisharat and M. Bastiaansen, Complexities related to the amorphous content of lactose carriers, *Int. J. Pharm.: X*, 2023, **6**, 100216.